

**AN EXPERIMENTAL STUDY OF FILTER LOADING WITH LIQUID
AEROSOLS**

G. Scott Earnest^a
Da-Ren Chen^b
David Y.H. Pui^b

^aU.S. Department of Health and Human Services
Public Health Service
Centers for Disease Control and Prevention
National Institute for Occupational Safety and Health
Division of Applied Research and Technology
4676 Columbia Parkway, MS-R5
Cincinnati, Ohio 45226

^bParticle Technology Laboratory
Mechanical Engineering Department
University of Minnesota
111 Church Street S.E.
Minneapolis, Minnesota 55455

Report Date:
January 2001

Report No.:
EPHB 218-05r

MANUSCRIPT EDITED BY:
Anne M. Votaw

MANUSCRIPT PREPARED BY:
Bernice L. Clark

To be published in American Industrial Hygiene Association Journal

An Experimental Study of Filter Loading with Liquid Aerosols
G. Scott Earnest, Da-Ren Chen, David Y.H. Pui

Abstract

Filter loading with liquid aerosols was studied experimentally for a variety of filters, liquids, and flow conditions. As fibrous filters were loaded with liquid aerosols, pressure drop and collection efficiency increased under most conditions studied. Pressure drop across the filter increased more rapidly when loaded with the same volume of high density and viscosity liquids, when compared to lower density and viscosity liquids. Early in the filter loading process, different liquids produced minor differences in filter pressure drops. However, as more liquid collected within the filter, the pressure drop differences increased.

Although collection efficiency generally increased with liquid loading, there were some notable exceptions. For filters, having low initial packing densities and made from materials that easily hold static charge, large drops in collection efficiency were observed for all particle sizes at a face velocity of 10 cm/sec. These drops in efficiency typically occurred when the pressure drop ratio was less than five. These collection efficiency results were explained in part by a loss of electrostatic charge, increased effective fiber diameter, and flow channeling within the filter. For face velocities above 50 cm/sec, collection efficiency increased for all particle sizes, throughout the loading process. Filters loaded with glycerol, a non-wetting liquid with the highest viscosity, tended to have higher collection efficiencies than filters loaded with other liquids under the same conditions. This was explained by liquid-fiber interaction. Basic mechanisms affecting both the filter pressure drop and collection

efficiency are presented in the paper, along with a discussion of liquid-fiber interaction.

Keywords: filtration, mists, filter loading, liquid aerosols, collection efficiency

A. Introduction

Much research has been devoted to understand the filtration process in fibrous filters. Most of the previous work has focused on the initial filtration process, when only small quantities of aerosols are collected on the filter surface. It is important not only to understand the initial parameters that affect filtration but also to be able to predict changes that may occur throughout the filtration process.

As filters are loaded with aerosols, their performance goes through dramatic changes. These changes can be different depending upon whether the filter is being loaded with solid or liquid aerosols. Filter loading with solid aerosols has been studied extensively, and many models have been developed to describe changes in pressure drop⁽¹⁻⁴⁾ and collection efficiency.⁽⁵⁻⁷⁾ However, this is not the case for liquid loading.

Despite less research, some liquid loading studies have been conducted. There are a variety of areas where filters may become loaded with liquid aerosols such as filters near metalworking fluid (MWF) operations (Leith, 1996; Raynor, 2000; Belden, 1994), coalescing filters in chemical processes,⁽⁸⁻¹¹⁾ engine crankcase filters, compressed gases,⁽¹²⁾ and related fields. Yet, a great deal remains to be learned about filter loading with liquids.

An experimental study was performed to evaluate changes in filter pressure drop and fractional collection efficiency as filters were loaded with liquid aerosols. A fundamental aspect of this study was the desire to look at a wide range of conditions. Many earlier studies in this area have

been limited in scope because they have examined a relatively small number of filters, liquids, and/or flow conditions.

B. Experimental System and Methodology

The present study was enhanced by an evaluation of the changes in performance for a variety of fibrous filters, as they were loaded with polydisperse dense mists. Test aerosols included organic liquids and MWFs to provide a range of physical properties. The organic liquids, used later for developing models, were relatively nonvolatile. Viscosities varied from approximately 20 to 1,500 centipoise at normal temperature and pressure. A wide range of flat-sheet filter media, consisting of fiberglass, polypropylene, polyester, and cellulose fibers was also tested.

Conventional and electret media were evaluated. Tables 1 and 2 provide a list of the liquids and filters that were evaluated and their properties. Face velocities ranged from 5 to 150 centimeters per second (cm/sec), and airflow through the filter was vertically downward and parallel to gravity.

Experimental System

Filter loading experiments were conducted using the Coarse Aerosol Filter Test System (CAFTS) of the Particle Technology Laboratory (PTL), Mechanical Engineering Department, University of Minnesota. This system, has been successfully used in other studies, and enables testing of air filters for their flow resistance, particle collection efficiency, and dust

loading behavior. The CAFTS system can be divided into four components:⁽¹³⁾ an air flow and cleaning system, a particle generation system, particle counting and sizing system, and computer-controlled data acquisition system. A diagram of the system is shown in Figure 1.

Airflow and cleaning system

A computer-controlled 230-volt blower provided airflow. Voltage was supplied to a Dayton® AC inverter, and voltage was modified based upon the desired fan speed. Air entered the system through a large pleated, high-efficiency particulate air (HEPA) filter to remove ambient particles before entering the upper plenum. An adjustable baffle inside of the plenum ensured proper mixing and uniform flow through the test duct.

The circular test duct had a cross-sectional area of approximately 100 square centimeters (cm²). The filter was held in the center of the test duct with an airtight filter holder. The filter holder had a stainless steel backing which was designed to support the filter during the loading process. Airflow was exhausted from the bottom plenum back into the HEPA filter bed, to remove particles from the exhaust, prior to recirculation. An orifice meter measured the airflow rate through the system. Several orifice meters, ranging in size from 0.2- to 4-in. diameter were used, based upon the desired airflow rate.

Two pressure taps, above and below the filter, measured the filter pressure drop. Two others measured the pressure drop across the orifice flow meter. Both sets of pressure drops were monitored by magnehelic gauges and measured automatically by electronic pressure transducers, which were connected to the computer. A feedback loop between the

computer and blower was used to maintain a constant face velocity through the filter during the loading process.

Particle generation system

Particles enter the experimental system through two ports near the top. Liquid aerosols were generated by two Collison-type atomizers, which passed compressed air at 10 to 40 pounds per square inch gauge (psig) past a bulk liquid held in a reservoir. These atomizers produce a constant and reproducible output, which is important for filter loading studies. High velocity air broke up the liquid into droplets and then resuspended the droplets as an aerosol.⁽¹⁴⁾

Exposing the aerosols to krypton-85 and polonium-210 sources, held inside of aluminum tubes, neutralized electrical charges on the aerosols. All aerosols passed through the tube prior to reaching the filter. The particles were brought to a state of Boltzmann charge equilibrium.⁽¹⁵⁾ The top of the neutralizer was tapered to minimize potential losses of large particles.

Particle counting and sizing system

The Hiac/Royco Model 5230 laser particle counter (LPC) was used for fractional collection efficiency measurements. This instrument samples at a flow rate of 0.2 cubic feet per minute (cfm) for particles in the 0.3 to 25 μm size range. There are eight channels with adjustable bin sizes. When using this counter, the coincidence limit was carefully observed. The system has several electric valves, which separate the counter and the test duct. Loading aerosol generation was temporarily stopped when the LPCs were used to make filter efficiency measurements. This prevented

the counter from being exposed to high aerosol concentrations that could quickly contaminate the optics. The counter being used was returned to the manufacturer for cleaning and calibration prior to beginning the study.

Aerosol sampling lines were located upstream and downstream of the test filter. The sampling lines have removable tips that allow mounting of various sized sharp-edged isokinetic probes. During the current study, only one counter was used to avoid the variability inherent from using two particle counters. Prior to beginning filter efficiency tests, the length and configuration of the upstream and downstream sampling lines were adjusted by counting upstream and downstream particles when no filter was in place to ensure similar particle losses. Additionally, an initial background efficiency measurement was made with no filter in place. The results were saved and used to correct subsequent efficiency measurements during filter testing.

Computer-controlled data acquisition system

The computer used an AD/DA card to control the blower speed and measure filter and orifice pressure drops. Programs were written in Labview® software to measure and record filter pressure drop and particle collection efficiency.

Potential sources of experimental error

This experiment was conducted in the laboratory where many sources of error that might be of concern in a field study can be more easily controlled. Experiments were conducted in a random order to attenuate the effects of variables that could not be controlled. Numbers were

assigned to each set of experimental conditions, and conditions were randomly selected and evaluated.

The experimental methodology was rigorously followed, and each test run followed the same procedures. For each run, filter efficiency measurements were taken for the clean filter, and efficiency measurements were made periodically as the filter was loaded. Each time a filter efficiency measurement was made, pressure drop across the filter was measured, and the collected filter mass was determined using an electronic microbalance. Sampling upstream and downstream of the filter each took approximately one minute, and sufficient time was provided between measurements to ensure that the sampling lines were thoroughly purged. Filter efficiency measurements for each condition were repeated several times. After each test run, the experimental system was thoroughly cleaned to reduce the effect of prior experiments influencing a subsequent one.

Other measurements

An NRD electrostatic field meter Model 520A (Grand Island, NY) was used in this study to measure the electrostatic potential for several conventional and electret test filters. The NRD electrostatic field meter is a full-functioned meter that uses distance-ranging lights to ensure accuracy and consistency of measurements. It has been calibrated to measure kilovolts per inch from +/- 19.99 KV, up to 59.99 KV at a three-inch distance to the filter.

Liquid-fiber interaction was qualitatively evaluated with the aid of an optical microscope connected to a digital camera and computer that used

Image® software to download the digital picture. All photographs were taken during stationary conditions when the filter was not being loaded or influenced by face velocity.

Experimental design

The dependent variables for this study were the pressure drop and collection efficiency. The independent variables are the liquid properties and face velocities. Experiments were conducted using a factorial design in which there were multiple levels for face velocity and loading liquids. This experimental design was used to evaluate how each of the independent variables affected the dependent variables and was repeated for different filters. The hypotheses that were tested can be stated as follows:

Is there a statistically significant difference in filter pressure drop for a filter being loaded with the same volume of liquid A as compared to other liquids for a given set of conditions?

Is there a statistically significant difference in filter collection efficiency for a filter being loaded with the same volume of liquid A as compared to other liquids for a given set of conditions?

Hypotheses were tested by performing analysis of variance (ANOVA) on the data by computing the sum of square values that measure the data variation. The F-ratio and p-value were calculated to determine the test significance at the 5% significance level. When the F-ratio was significant, the least significant differences (LSD) multiple range test was applied, to compare the means between groups.

C. Experimental Results

Experimental results are described in the next several sections. Pressure drop results are presented first, followed by fractional collection efficiency, electrostatic charge, and liquid-fiber interaction results.

Pressure Drop Results

Pressure drop across a filter is typically quite low compared to atmospheric pressure, and air can therefore be assumed to be incompressible. Flow through the filter is dominated by viscous forces, and Reynolds number may be assumed to be small.⁽¹⁶⁾ Pressure drop across a filter is proportional to the thickness L , air velocity u , fiber diameter d_f , viscosity of air μ_{air} , and packing density α . In simple terms this can be stated as follows: the pressure drop across a filter is proportional to the rate of fluid flow through the filter and has been defined by Darcy's Law, a fundamental filtration equation:

$$\Delta P = \frac{\alpha L u \mu_{\text{air}}}{d_f^2} \quad (1)$$

A useful way to compare filter pressure drop during loading with liquid aerosols is to plot the pressure drop ratio $\Delta P/\Delta P_i$, versus the revised packing density α' . The pressure drop ratio and revised packing density are dimensionless numbers. The pressure drop ratio $\Delta P/\Delta P_i$, represents the current pressure drop across the filter ΔP as the filter is loaded, divided by the initial pressure drop across the clean filter ΔP_i . The

pressure drop ratio of a clean filter is equal to one because ΔP and ΔP_i are initially the same.

The revised packing density α' , is a parameter used to express the volume of liquid collected within the structure of the filter relative to the initial packing density α . All filters have an initial filter packing density that represents the volume of the total filter occupied by fibers. Filter packing density is defined as

$$\alpha = \frac{m_f}{\rho_f L} \quad (2)$$

Where m_f is the filter basis weight in milligrams per square centimeter (mg/cm^2) and ρ_f is the fiber density in g/cm^3 . For filters tested as part of this investigation, packing densities ranged from approximately 0.02 to 0.10. This indicates that between 2% and 10% of the volume of the filters were occupied by fibers. The revised packing density, then, uses the fiber volume from the filter's initial packing density, and adds the volume of collected liquid to that value. This value is divided by the volume of the entire filter structure. The revised packing density, as used in this study, is defined by the following equation:

$$\alpha' = \frac{V_{\text{fib}} + V_{\text{liq}}}{V_{\text{filter}}} \quad (3)$$

Thus, for a given mass of liquid, liquids with a higher density occupy a smaller volume than liquids having a low density.

A close examination of the filter pressure drop results from the present study reveals a relatively consistent pattern that occurs for nearly all conditions studied, regardless of the filter or flow conditions. This data trend can be seen in Figure 2. This figure plots the pressure drop ratio on the y-axis versus the revised packing density on the x-axis.

Using these axes, the typical shape of the curve generated when loading filters with liquid aerosols was similar to either a power or sigmoid function depending upon the degree of loading. As the filter was loaded, initially, there was a relatively gradual increase in pressure drop, followed by a rapid rise until the filter approached saturated conditions, at which time the pressure drop began to stabilize. For a given liquid and filter type, saturation occurred at lower revised packing densities as the face velocity increased. The increased flow rate and corresponding pressure prevented the filter from retaining the same volume of liquid. Similarly, for a given filter type and loading liquid, the pressure drop ratio is higher for the same revised packing density at higher face velocities. Pressure drop ratios for these data were usually below 50; however, pressure drop ratios exceeding 50 sometimes occurred when the initial filter pressure drop was extremely small because of low face velocities and low, initial, filter, packing densities.

Another clear trend is that for a given filter and revised packing density, the pressure drop ratio tends to be higher for glycerol and castor oil than other liquids. Glycerol and castor oil have considerably higher viscosities and surface tensions than the other liquids evaluated in this study. Likewise, the density of glycerol was highest, followed by castor oil.

Figure 3 is a plot of the pressure drop ratio versus the revised packing density for a polypropylene filter loaded with several MWFs. The MWFs had similar physical properties, and their viscosities ranged from 10 to 181 centipoise (cp). Alternatively, the simple fluids tested had viscosities ranging from 23 to 1,500 cp. Pressure drop ratios were comparable for filters that were loaded with different MWFs. Although Figure 3 is for a polypropylene filter loaded at a face velocity of 50 cm/sec, similar results were obtained for different filter types and flow conditions. In addition to the MWFs, heavy mineral oil was plotted on this graph because its physical properties were very similar to the metalworking fluids evaluated. Each of these MWFs, with like physical properties, behaved in a manner consistent to heavy mineral oil.

Fractional Collection Efficiency Results

Changes in fractional collection efficiency during loading are much more complex than changes in filter pressure drop. Part of the reason for this complexity is that, unlike filter pressure drop, fractional collection efficiency sometimes decreases during the liquid loading process. Fractional collection efficiency is influenced by a wide variety of mechanisms including diffusion, interception, impaction, gravitation, and electrostatics. The relative influence of each of these mechanisms may change during the loading process. Similar to the filter pressure drop results discussed earlier, fairly clear trends can be observed by examining all of the filter fractional collection efficiency results.

Despite some transitory drops in efficiency during the current study, fractional collection efficiency generally increased as the filters were loaded with liquid aerosols. Commonly, there was a more rapid rise in efficiency as the filter was loaded with glycerol, as compared to other test liquids. Collection efficiencies usually increased with loading, but there were some exceptions.

In Figures 4 to 6, the fractional collection efficiency is plotted on the y-axis versus the particle diameter in micrometers as measured with an LPC, on the x-axis. The LPC provides an estimate of the geometric mean particle size based upon the intensity of scattered light. Each datum series displayed on the graphs represents several efficiency measurements taken under different loading conditions. Each loading condition corresponds to a different pressure drop ratio, shown in the legend on the right-hand side.

Figures 4 to 6 depict the three primary trends in collection efficiency results observed during this study. In Figure 4, collection efficiency generally increases or sometimes remained relatively constant for all particle sizes as the filter was loaded. In Figure 5, there is a large (15-20%) dip in efficiency for submicron particle sizes during the loading process. In Figure 6, collection efficiency drops nearly 30% for all particle sizes until a bottom is reached, and collection efficiency eventually begins to increase.

Trends in the filter collection efficiency were strongly influenced by the face velocity. Filters were tested at face velocities ranging from 5 to 150 cm/sec. For all conditions studied, when face velocities exceeded 50

cm/sec, the fractional collection efficiency increased at all particle sizes. Under high face velocity conditions, there were no drops in efficiency observed. For face velocities of 50 cm/sec and below, transitory drops in collection efficiency were observed. Sometimes these drops in efficiency occurred at all particle sizes, and other times, the efficiency drops occurred only for submicron particles.

As the face velocity was reduced, drops in efficiency became more profound, sometimes occurring at all particle sizes. There also appeared to be a correlation between initial packing density of the filter, and the likelihood that a drop in efficiency would occur. Filters with lower packing densities were more likely to experience a drop in efficiency during the liquid loading process. The trends that are described above and shown in Figures 4 to 6 were relatively consistent regardless of the loading liquids. These same trends were repeated when the filters were loaded with MWFs.

Statistical Analysis of Pressure Drop and Collection Efficiency Results

Statistical analysis was performed on the experimental data. Dependent variables were the filter pressure drop and collection efficiency, and independent variables were the loading liquids. Statistical analysis was used to evaluate how the independent variables affect the dependent variables by testing two hypotheses as described earlier.

Results of the statistical analysis are discussed below. Filter pressure drop and collection efficiency data were analyzed and grouped according to the revised packing density. Wet-laid fiberglass filters loaded with different liquids, at the same face velocity and revised packing density, were compared. Data for each loading condition was collected during four independent experimental runs.

Statistically significant differences were found between filter pressure drops for a filter loaded with the same volume of different liquids for a given set of conditions. Similarly, statistically significant differences were found between filter collection efficiencies for a filter loaded with the same volume of different liquids for a given set of conditions. Although there were statistically significant differences in filter pressure drops and collection efficiencies between loading liquids, those differences were not universal. Rather, the differences manifested themselves gradually, and the differences increased as loading continued.

For example, by comparing filter pressure drop results at a revised packing density of 0.10, the filter pressure drop for glycerol loading was statistically significantly different from the filter pressure drop for loading with other liquids. However, at the same revised packing density, the filter pressure drops resulting from the other loading liquids, DOS, HMO, and castor oil, were not significantly different from each other. As loading continued, castor oil became statistically significantly different from DOS and HMO. Eventually, at higher revised packing densities of 0.30, the filter pressure drops for each loading liquid were significantly different from each other.

Statistical analysis of the total filter collection efficiency found that there were differences in efficiencies among all loading liquids at revised packing densities as low as 0.10. These efficiency differences increased as filter loading progressed. Differences in total efficiency occurred despite the narrower ranges between collection efficiencies as compared to pressure drops. At a face velocity of 50 cm/sec, mean filter collection efficiencies ranged from 0.0625 for DOS, $\alpha' = 0.10$ to 0.8625 for castor oil, $\alpha' = 0.30$. At a face velocity of 50 cm/sec, mean filter pressure drops ranged from 0.315 inches of water for heavy mineral oil, $\alpha' = 0.10$ to 4.265 inches of water for castor oil, $\alpha' = 0.30$.

Electrostatic Charge Results

A test was conducted to determine the effect of static charge on the drop in collection efficiency in Figure 6. The data in Figure 6 was gathered for a conventional, polypropylene filter loaded with heavy mineral oil at 10 cm/sec. A polypropylene filter, a material that holds static charge readily, was submerged completely in isopropyl alcohol and dried for hours to remove any residual charge. Figure 7 shows that when the filter was tested under the same conditions, dramatic differences were found. The drop in collection efficiency that occurred in Figure 6 disappeared in Figure 7 because the static charge on the filter was removed prior to loading. It was also discovered that collection efficiency degradation for electret media was quite similar to conventional polypropylene media (Figure 6) loaded under the same conditions.

Figure 8 shows data from the experiments described above. Total fractional collection efficiency determined on the basis of the measured particle sizes is plotted on the y-axis, and the pressure drop ratio is plotted on the x-axis. Clearly the uncharged polypropylene filter that was dipped in isopropyl alcohol did not experience the dramatic drop in efficiency, as did the normal polypropylene filter. The initial collection efficiency was much lower than with the normal filter because residual charge on the fibers was degraded.

In Figure 9, electrostatic charge was evaluated on conventional and electret filter media. Conventional filters are shown on the left side of the graph, and electret media are displayed on the right. This graph shows that the electret media has a larger absolute, electrostatic potential than the conventional media had; however, the media could be positively or negatively charged. By monitoring changes in electrostatic potential of the filter during loading, it was possible to show how penetration increased (Figures 10 and 11) as electret and conventional filters were loaded at a face velocity of 10 cm/sec.

Liquid-Fiber Interaction Results

Different combinations of liquid-fiber interaction were evaluated based upon the observed contact angle. Contact angle, θ , describes the angle formed between a flat surface and a line originating at the contact point of the solid, liquid, and air drawn tangent to the surface of the droplet, as shown in Figure 12. If θ is less than or equal to 90° , the drop is said to "wet" the surface. If θ is greater than 90° , the liquid is "nonwetting." The

contact angle between a liquid and fiber is influenced by surface energies, roughness, heterogeneity, and temperature.

Three different liquid shapes were observed during this evaluation: unduloid, clamshell, and complete wetting. The clamshell shape was the only nonwetting shape observed. Observation of these three shapes is consistent with other studies.^(17, 19) Each of these shapes can be seen in Figure 13.

When the unduloid shape was observed on fibers, complete wetting, having a contact angle of zero, was also frequently seen. Typically, when loading with glycerol, the clamshell shape was observed. In the clamshell, the liquid does not completely surround the fiber. A summary of the liquid-fiber interactions for several of the evaluated liquid-fiber combinations is shown in Figure 14. Based upon experimental results, formation of the clamshell shape was associated with higher collection efficiencies than the other observed shapes.

D. Discussion

Pressure Drop Discussion

For early loading conditions, there did not appear to be major differences among pressure drop ratios for different liquids. However, as loading continued and the revised packing densities increased, a divergence in pressure drop ratios began to occur for different liquids. This divergence

manifested itself at lower revised packing densities when increasingly higher face velocities were used.

If one considers these results from a microscopic view, what seems to have happened is that, initially, such a small volume of liquid collected on the fibers that the liquid was relatively stationary. Because low and medium efficiency filters are inhomogeneous, the particles first collected on the most efficient portions of the filter. As more and more liquid collected within the filter, the interstitial air velocity increased. In time, small particles began to coalesce and form larger droplets that subsequently blocked the most efficient portions of the filter. As the pressure drop increased with loading, liquid films covering the largest fiber meshes were broken and air flowed through.⁽¹⁹⁾

Early in the collection process, liquid aerosols behaved similarly to solid particles because they simply divert the airflow, much as a solid particle would have done. However, as liquid aerosols continued to collect within the structure of the filter they eventually coalesced and became larger droplets. As the filter pressure drop increased and larger globules formed, the airflow eventually began to force the collected liquid through the filter. At this point, in this highly dynamic process, pressure drop ratios began to diverge for the different liquids. The divergence can be attributed to the fact that liquids with higher viscosities and densities are more resistant to flow.

It is important to remember that for organic liquids, used exclusively in this study, there was a direct correlation between viscosity and surface tension. Liquids having high viscosity strongly resist the force exerted by

the interstitial airflow and prefer to remain stationary, while less viscous liquids flow through a filter more readily. Many approaches may be followed to model these filter pressure drop results, and several of those approaches are outlined by Earnest.⁽²⁰⁾

Fractional Collection Efficiency Discussion

Fractional collection efficiency results are influenced by many factors. For the particle sizes and face velocities tested in this study, particle collection was dominated by the impaction and interception mechanisms. Unlike solid particles, liquid aerosols generally do not experience particle bounce.^(21, 22) When collection by impaction plays a dominant role, density of the challenge aerosol can be important.⁽²³⁾ For example, glycerol has a much higher density than heavy mineral oil (1.26 g/cm³ vs. 0.87 g/cm³). When using geometric diameters, the higher density results in a higher Stokes number, which increases collection by impaction. Stokes number is defined as:

$$\text{Stk} = \frac{\tau u}{d_f} = \frac{\rho_p d_p^2 C_c u}{18 \mu_{\text{air}} d_f} \quad (4)$$

A few simple calculations of single fiber collection efficiency by impaction shows that for certain conditions, collection efficiency may differ by 10% because of differences in challenge aerosol densities.

As the filters were loaded in this study, interstitial velocities increased with the revised packing density because the flow remained constant as the

cross-sectional area within the filter was reduced. Increases to interstitial velocity will increase collection by impaction. Heavy mineral oil and oils with similar properties wetted the fibers; however, glycerol was generally nonwetting. Fibers wetted with heavy mineral oil may have behaved as if they had a larger effective diameter. If packing density remained constant, large diameter fibers would be less effective at capturing particles, as expressed in the following relationship for total filter collection efficiency.⁽²⁴⁾

$$\eta_t = 1 - e^{\left(\frac{-4\alpha\eta_s L}{\pi d_t}\right)} \quad (5)$$

Larger diameter fibers, increases in interstitial velocity, and Stokes number may all play some role in efficiency increase rates, particularly at high face velocities.

Several studies have documented drops in efficiency at low face velocities. However, unlike the current study, these drops in efficiency typically occurred for submicrometer particles, and there was no mention that efficiency increased as loading progressed. Drops in efficiency have been previously explained by increased interstitial velocities, thicker liquid-coated fibers, fewer fibers available for particle capture, filter structure alterations, and blocking portions of the filter.^(25, 26) While each of these explanations may play some role under certain conditions, other explanations should also be considered.

The current study focused on the transition from clean to saturated conditions; whereas, many earlier studies did not address the incremental

changes that occur during the transition. Instead, many prior studies compared clean to saturated conditions without thoroughly evaluating the transitional stage, a period when the largest drops in efficiency may have occurred. The present study found that it was precisely during the transition, when the pressure drop ratio was between 1.5 and 5 that the largest drops in collection efficiency occurred. Figure 15 shows transitional drops in the total collection efficiency for all measured particle sizes versus the pressure drop ratio.

Filter orientation with respect to gravity may also have influenced the results by changing the saturation point. In the majority of earlier studies, filters were positioned vertically rather than horizontally, and airflow through the filter was perpendicular rather than parallel to gravity. Filter orientation with respect to gravity affects the airflow pattern through the filter during the liquid loading process.⁽²⁷⁾

Filters oriented so that airflow through them is perpendicular to gravity, are likely to have increased airflow near the top of the filter and large blocking effects near the bottom where the liquid naturally drains. Likewise, if airflow through the filter were perpendicular rather than parallel to gravity, a greater percentage of fiber axes would be more closely aligned with the force of gravity. This natural orientation should enhance liquid drainage from the filter, which would, in turn, lower the revised packing density required to reach saturation and the corresponding filter pressure drop. If filter saturation were able to occur at lower revised packing densities, then it is possible that increases in collection efficiency, which might follow an initial drop would never occur. The current study typically had filters reach revised packing densities that were higher ($\alpha' = 0.50$ for low viscosity

liquids at low face velocities) than seen in previous studies where flow through the filter was perpendicular to gravity. The higher revised packing densities may help to explain why the current study had pressure drop ratios over two times greater than found in many other studies.

Finally, other studies have not evaluated as many filters or fiber types of as wide a range of packing densities, particularly polypropylene fibers, which are capable of holding a large static charge. The current study found that low packing density filters or filters that may have relied heavily on the electrostatic collection mechanism experienced dramatic drops in collection efficiency. Figure 16 is a plot of three polyester-glass fiber filters loaded with dioctyl-sebacate (DOS) at 10 cm/sec. Filter H, which experiences a drop in total collection efficiency has the lowest packing density of the three filters used.

Charge Effects Discussion

Charge loss was found to play an important role in the collection efficiency degradation observed in this study. Electrically charged filter media are extremely useful for producing a high capture efficiency and low-pressure drop. This type of media works well for capturing solid particles; however, the electrical charge degrades during loading, especially with liquid aerosols. The electrical field within the filter is strongest near the fiber and falls in strength as distance increases. Filters that depend on electrostatic attraction are more effective at lower velocities. The following equation for single fiber efficiency of the electrostatic image force, outlined by Davies,⁽²⁸⁾ shows that collection efficiency increases as velocity falls.

$$\eta_q = \left(\frac{\varepsilon - 1}{\varepsilon + 1} \right)^{1/2} \left(\frac{q^2}{3\pi\mu d_p d_f^2 u (2 - \ln Re_f)} \right) \quad (6)$$

Many conventional filters hold a charge on the fiber surface, which enhances collection efficiency, at low face velocities. As the filter is loaded with liquid aerosols, the natural charge may be degraded.⁽²⁹⁾ The extent of charge deterioration likely depends upon the loading liquid properties and liquid-fiber interaction.⁽³⁰⁾ One study has indicated that conducting oil will reduce the fiber charge, but insulating oil may increase the fiber charge.⁽³¹⁾ Wetting liquids that are capable of spreading rapidly on the fiber surface may cause the fiber charge and collection efficiency to drop more rapidly than a non-wetting liquid. Charge shielding can have a detrimental effect on the fractional collection efficiency at all particle sizes. This may explain the results in Figure 6, where the collection efficiency initially falls for all particle sizes. Eventually when the charge has dissipated and the filter is sufficiently filled with collected liquid, the efficiency begins to increase because other mechanical collection mechanisms become dominant. Clearly, when comparing the conventional media in Figure 9, the polypropylene filter has the largest absolute potential.

Charges on fiber filters can be dissipated by several mechanisms, including: conduction through the atmosphere, conduction through contacting bodies, and conduction on the surface of contacting bodies. Medley has shown that the charge on the surface of a fiber assembly such as a filter, decreases exponentially when the fibers are coated with a surface finish according to the equation:⁽³²⁾

$$q = q_0 e^{\left(\frac{-k\delta}{\varepsilon\varepsilon_0u}\right)} \quad (7)$$

Where q is the charge or charge density, q_0 is the charge transfer, k is the liquid conductivity, ε is the dielectric constant of the liquid, ε_0 is the permittivity of free space, u is the velocity that the material moves, and δ is the length of the liquid wedge formed at the point where the filter departs from the object rubbed.

Liquid-Fiber Interaction Discussion

Interaction between the liquid and fiber plays a fundamental role in determining the filter pressure drop and collection efficiency. Many factors influence how the loading liquid and filter fibers interact when they come into contact. The chemical and physical properties of both the liquid and fibers are of paramount importance. One of the most essential aspects of liquid-fiber interactions effecting filter behavior is fiber wettability.^(27, 33)

Liquids that wet a solid surface have a tendency to spread out, while non-wetting liquids will "ball up." In general, liquids with low surface tensions tend to wet most surfaces. Fibers vary in wettability, and are influenced by many different factors. For this reason, wettability of fibers can be complex, involving subtle differences that complicate studies. For example, cotton fibers that have been contaminated with wax are difficult to wet, whereas scoured or bleached cotton is wetted easily. The arrangement of fibers within the filter may also influence the wettability.

Fibers oriented in a parallel manner form a system of capillaries wetted more easily than fibers in a random arrangement.⁽³⁴⁾

Droplets may form many different stable angles on a solid surface, and a variety of contact angles were observed on the same fiber during this study. In general, for most of the liquid-fiber combinations in this study, different forms of the unduloid shape were observed on the fiber surface. An unduloid is the hydrodynamically stable shape formed by rotating an elliptical cycloid around its axis.⁽¹⁷⁾ It meets the Laplace requirements for stability and completely surrounds the fiber surface. The contact angle for the unduloid may vary between 0-90°, based upon a variety of factors outlined by Roe.⁽¹⁸⁾ The shape that is assumed by the liquid depends not only on the contact angle, but also on the volume of the liquid relative to the volume per unit length of the fiber.

Liquids with strong hydrogen bonding, such as glycerol, tend to have high surface tensions, which causes them to be nonwetting on the surface of most fibers. The other loading liquids had weaker secondary bonds and, in most cases, were found to wet the fiber easily. As observed during this study, nonwetting liquids were more likely to have higher collection efficiencies than wetting liquids. This observation is consistent with the findings of Fairs.⁽⁹⁾ There are several possible explanations for the effect. Total wetting or the unduloid shape more readily removes surface charge on the fiber and increases the effective fiber diameter. The clamshell shape forms when the liquid does not spread or is nonwetting, so greater charge will likely be retained on the fiber and much of the fiber diameter remains the same.

F. Conclusions

An experimental study was conducted to evaluate how liquid loading affected filter performance for a variety of conditions. During the early stages of the loading process, there was not a great deal of difference between filter pressure drops, regardless of the physical properties of the loading liquid. As more and more liquid aerosols collected within the filter the liquid properties began to play increasingly important roles, and the pressure drops diverged as a consequence of the liquid properties. These differences were found to be statistically significantly different on the basis of ANOVA and LSD multiple comparison tests. Filters that have been loaded with higher viscosity liquids generally have higher-pressure drops for the same revised packing densities.

Filter fractional collection efficiencies also changed during the loading process. Although the overall trend for fractional collection efficiency was up during the loading process, substantial, drops in efficiency were observed under certain loading conditions. Transitional drops in fractional collection efficiency were noted when face velocities and filter packing densities were low and when the electrostatic collection mechanism played an important role in the collection process. For the conditions described above, fractional collection efficiency was observed to drop for all particle sizes.

At face velocities above 50 cm/sec, fractional collection efficiency typically rose for all particle sizes. When conventional filters that did not hold a substantial electrostatic charge were tested at low face velocities, it was common to observe a transitional drop in collection efficiency for

submicron-sized aerosols, while the efficiency for larger aerosols increased. Filters loaded with MWFs behaved similar to HMO or DOS that have similar physical properties to the MWFs tested. Finally, there were three general liquid shapes observed on the fiber surface: unduloid, clamshell, and complete wetting. The clamshell shape was associated with higher collection efficiencies. Similar to the pressure drop results, statistical analysis showed that total collection efficiencies were significantly different for the different loading liquids.

G. Acknowledgments

This research is partially supported by the Center for Filtration Research at the University of Minnesota. Center Members include 3M Company, AAF International, Donaldson Company, Fleetguard Nelson, Inc., Honeywell, TSI Inc., W.L. Gore and Associates, and Filtrauto. We would also like to thank Dr. Dennis O'Brien and other managers in the National Institute for Occupational Safety and Health, Division of Applied Research and Technology for their support of Mr. Earnest during his long-term training tenure at the University of Minnesota, Particle Technology Laboratory.

H. Nomenclature

C_c Cunningham slip correction factor
 d_f fiber diameter, μm
 d_p particle diameter, μm

F_d	drag force on unit length of cylinder perpendicular to airflow, dynes/cm
g	gravitational acceleration
i,j,k	x, y, or z direction of the three dimensional coordinates
k	conductivity of the liquid
K	Boltzmann's Constant
L	filter thickness, cm
L_f	specific fiber length (length of fiber per unit volume), cm/cm ²
m_f	filter basis weight (weight per unit filter area), g/cm ²
N	particle concentration
N_{cap}	capillary number
N_G	gravitational parameter
ΔP	pressure drop, inches H ₂ O
ΔP_i	initial pressure drop across filter, inches H ₂ O
ΔP_s	pressure drop across filter at saturated state, inches H ₂ O
P	filter penetration, (1- η)
q	charge on the particle
q_0	charge transfer
Re	flow Reynolds number
Re_f	fiber Reynolds number
Stk	Stokes number
u_i	interstitial air velocity inside the filter media, cm/s
u	superficial air velocity, cm/s
V_{fib}	fiber volume
V_{fil}	volume of the entire filter
V_{liq}	volume of the collected liquid

Greek Symbols

α	filter packing density
α'	filter packing density modified for retained liquid
ϵ	dielectric constant
ϵ	permittivity of free space
η_t	total filter efficiency
η_q	single fiber efficiency for electrostatics
η_s	total single fiber efficiency
θ	liquid/fiber contact angle
σ	surface tension
σ_g	geometric standard deviation of particle distribution
μ	liquid viscosity, Poise

μ_{air}	air viscosity, Poise
π	ρ_i
ρ_l	liquid density, g/cm ³
ρ_a	air density, g/cm ³
ρ_f	fiber density, g/cm ³
ρ_p	particle density, g/cm ³
τ	relaxation time

I. Tables

Table 1. Test Aerosols (Simple Liquids) and Their Physical Properties

<i>Aerosol</i>	<i>Density, g/cm³</i>	<i>Viscosity, cpoise</i>	<i>Surf. Tension, dynes/cm</i>
Diocetyl-sebacate (DOS)	0.914	23.0	31.3
Diocetyl-phthalate (DOP)	0.981	80.0	30.9
Lite Mineral Oil (LMO)	0.833	13.8	29.9
Heavy Mineral Oil (HMO)	0.870	30.8	31.6
Castor Oil	0.969	986.0	35.1
Glycerol	1.26	1490.0	63.4

Table 2. Experimental Filter Media and Their Properties

<i>Media</i>	<i>Material</i>	D_f , μm	ρ_f , g/cm^3	L , <i>cm</i>	m_f , mg/cm^2	<i>Vel</i> (<i>cm/s</i>) vs. Δp "H ₂ O	<i>Packing</i> <i>density,</i> α
A	Polyester Glass	12 5	1.38 2.1	0.0927	10.96	50 cm/sec 0.16"	0.0724
B	Wetlaid Fiber Glass	4.6	2.1	0.0746	7.60	100 cm/s 0.78"	0.0485
C	Polypropylene	12.0	0.91	0.1273	11.62	250.81 cm/s 1.66"	0.1003
D	Cellulose	20.0	1.52	0.1510			0.035
E	Cotton Polyester	20.0 12.0	1.52 1.38	0.1507	7.67	148.09 cm/s 0.16"	0.0351
F	Glass	6.4	2.1	0.2446	9.13	250.73 cm/s 1.31"	0.0177
G	Polyester Glass	10 2	1.38 2.1	0.0998	14.76	50 cm/s 1.34"	0.0930
H	Polyester Glass	12 5	1.38 2.1	0.1194	8.01	50 cm/s 1.75"	0.0414
I	Electret Polypropylene		0.91	0.1399	4.25	10 cm/s 0.049"	0.0264
J	Electret Polypropylene		0.91	0.1770	3.73	10 cm/s 0.031"	0.0293
K	Electret Polypropylene/ Polyester		0.91	0.0058	3.16	10 cm/s 0.061"	0.4758

J. References

1. **Kanaoka, C., Hiragi, S.:** Pressure Drop of Air Filter with Dust Load. *Journal of Aerosol Science* 21(1):127-137 (1990).
2. **Fuchs, N.A., Kirsch, A.A.:** Studies on Fibrous Aerosol Filters - II, Pressure drop in Systems of Parallel Cylinders. *Ann. Occu. Hyg.* 10:22-23 (1967).
3. **Juda, J., and S. Chrosciel:** A Theoretical Model of Pressure-Loss Increase During the Filtration Process. *Staub-Reinhalt. Luft* 30(5):12-15 (1970).
4. **Kirsch, A.A., Fuchs, N.A.:** Studies on Fibrous Aerosol Filters--II. Pressure Drop in Systems of Parallel Cylinders. *Ann. Occup. Hyg.* 10:23-30 (1967).
5. **Lee, K.W., and B.Y.H. Liu:** Theoretical study of aerosol filtration by fibrous filters. *Aerosol Sci. Technol.* 1(2):147-162 (1982).
6. **Brown, R.C.:** A many-fibre model of airflow through a fibrous filter. *J. Aerosol Sci.* 15(5):583-594 (1984).
7. **Gentry, J.W., and K.R. Choudhary:** Collection efficiency and pressure drop in grid filters of high packing densities at intermediate Reynolds numbers. *J. Aerosol Sci.* 6(5):277-290 (1975).
8. **Brink, J.A., Burgrabe, W.F., Greenwell, L.E.:** Mist Eliminators for Sulfuric Acid Plants. *Chemical Engineering Progress* 64(11):82-86 (1968).
9. **Fairs, G.L.:** High Efficiency Fibre Filters for the Treatment of Fine Mists. *Trans. Instn. Chem. Engrs.* 36:476-485 (1958).
10. **Claes, J., DeBruyne, R.:** Demisting with Metal Fibre Webs and Felts *Filtration Society's Conference on Dust Control and Air Cleaning* 1975:9-13.
11. **York, O.H., Popele, E.W.:** Wire Mesh Mist Eliminators. *Chemical Engineering Progress* 59(6):45-50 (1963).

12. **Brink, J.A., Burggrabe, W.F., Greenwell, L.E.:** Mist Removal from Compressed Gases. *Chemical Engineering Progress* 62(4):60-65 (1966).
13. **Poon, W.S., B.Y.H. Liu, and N. Bugli:** Experimental Measurement of Clean Fractional Efficiency of Engine Air Cleaning Filters. *Society of Automotive Engineers Technical Papers Series* 96MJA381 (1996).
14. **Lefebvre, A.H.:** *Atomization and Sprays*. New York: Taylor and Francis Publishers, 1989.
15. **Cooper, D.W., Reist, P.C.:** Neutralizing Charged Aerosols with Radioactive Sources. *Journal of Colloid and Interface Science* 45(1):17-27 (1973).
16. **Brown, R.C.:** *Air Filtration: An Integrated Approach to the Theory and Application of Fibrous Filters*. Oxford, England: Pergamon Press, 1993.
17. **Minor, F.W., Schwartz, A.M.:** The Migration of Liquids in Textile Assemblies-Part III The Behavior of Liquids on Single Textile Fibers. *Textile Research Journal* 29(12):940-949 (1959).
18. **Roe, R.J.:** Wetting of Fine Wires and Fibers by a Liquid Film. *Journal of Colloid and Interface Science* 50(1):70-79 (1975).
19. **Yoshida, T., Kousaka, Y., Inake, S., Nakai, S.:** Pressure Drop and Collection Efficiency of an Irrigated Bag Filter. *Ind Eng. Chem., Process Des. Dev.* 14(2):101-105 (1975).
20. **Earnest, G.S.:** "A Fundamental Study of Filter Loading with Liquid Aerosols." Ph.D., University of Minnesota, 2000.
21. **Ellenbecker, M.J., D. Leith, and J.M. Price:** Impaction and Particle Bounce at High Stokes Numbers. *Journal of the Air Pollution Control Association* 30(11):1224-1227 (1980).
22. **First, M.W., and W.C. Hinds:** High Velocity Filtration of Submicron Aerosols. *Journal of the Air Pollution Control Association* 26(2):119-123 (1976).

23. **May, K.R., and R. Clifford:** The Impaction of Aerosol Particles on Cylinders, Spheres, Ribbons and Discs. *Ann. Occup. Hyg.* 10:83-95 (1967).
24. **Hinds, W.C.:** *Aerosol Technology: Properties, Behavior, and Measurement of Airborne Particles.* New York: Wiley, 1982.
25. **Payet, S., Bouland, D., Madelaine, G., Renoux, A.:** Penetration and Pressure Drop of a HEPA Filter During Loading with Submicron Liquid Particles. *Journal of Aerosol Science* 23(7):723-735 (1992).
26. **Conder, J.R., Liew, T.P.:** Fine Mist Filtration by Wet Filters -II: Efficiency of Fibrous Filters. *Journal of Aerosol Science* 20(1): 45-57 (1989).
27. **Agranovski, I.E., and R.D. Braddock:** Filtration of Liquid Aerosols on Wettable Fibrous Filters. *AIChE Journal* 44(12):2775-2783 (1998).
28. **Davies, C.N.:** *Air Filtration.* New York: Academic Press, 1973.
29. **Kanaoka, C., H. Emi, and T. Ishiguro:** Time Dependency of Collection Performance of Electret Filter. In: Liu BYH, Pui DYH, Fissan HJ, eds. *Aerosols: Science, Technology, and Industrial Applications of Airborne Particles.* New York: Elsevier Science, 1984; 613-616.
30. **Feltham, F.J.:** The Hansen Filter. *Filtration and Separation* July/August:370-372 (1979).
31. **Morton, W.E., and J.W.S. Hearle:** *Physical Properties of Textile Fibers.* Manchester, U.K.: The Textile Institute, 1993.
32. **Medley, J.A.** *Journal of the Textile Institute* 45:T123 (1954).
33. **Agranovski, I.E., Braddock, R.D.:** Filtration of Liquid Aerosols on Nonwetable Fibrous Filters. *AIChE Journal* 44(12):2784-2790 (1998).
34. **Minor, F.W., Schwartz, A.M., Wulkow, E.A., Buckles, L.C.:** The Migration of Liquids in Textile Assemblies-Part II The Wicking of Liquids in Yarns. *Textile Research Journal* 29(12):931-939 (1959).

K. List of Figures

Figure 1. Test System Diagram.

Figure 2. Polyester-glass Fiber Filter (Filter A) Loaded with Aerosols at 50 cm/sec (Pressure Drop Ratio versus Revised Packing Density).

Figure 3. Pressure Drop Ratio versus Revised Packing Density for a Polypropylene Filter Loaded with MWF and Heavy Mineral Oil at 50 cm/sec (Pressure Drop Ratio versus Mass Loading).

Figure 4. Wet-laid fiberglass Filter Loaded with DOS at 100 cm/sec (Fractional Collection Efficiency versus Particle Diameter).

Figure 5. Polypropylene Filter Loaded with Caster Oil at 50 cm/sec (Fractional Collection Efficiency versus Particle Diameter).

Figure 6. Polypropylene Filter Loaded with Heavy Mineral Oil at 10 cm/sec (Fractional Collection Efficiency versus Particle Diameter).

Figure 7. Decharged Polypropylene Filter Loaded with Heavy Mineral Oil at 10 cm/sec.

Figure 8. Comparison of Total Fractional Collection Efficiency for a Normal and Uncharged Polypropylene Filter with Heavy Mineral Oil at 10 cm/sec.

Figure 9. Comparison of the Initial Static Potential for Several Different Conventional and Electret Test Filters.

Figure 10. Effect of Mass Loading with Heavy Mineral Oil on the Surface Potential and Total Penetration of an Electret Filter at 10 cm/sec.

Figure 11. Effect of Mass Loading with DOS on the Surface Potential and Total Penetration of a Polypropylene Filter at 50 cm/sec.

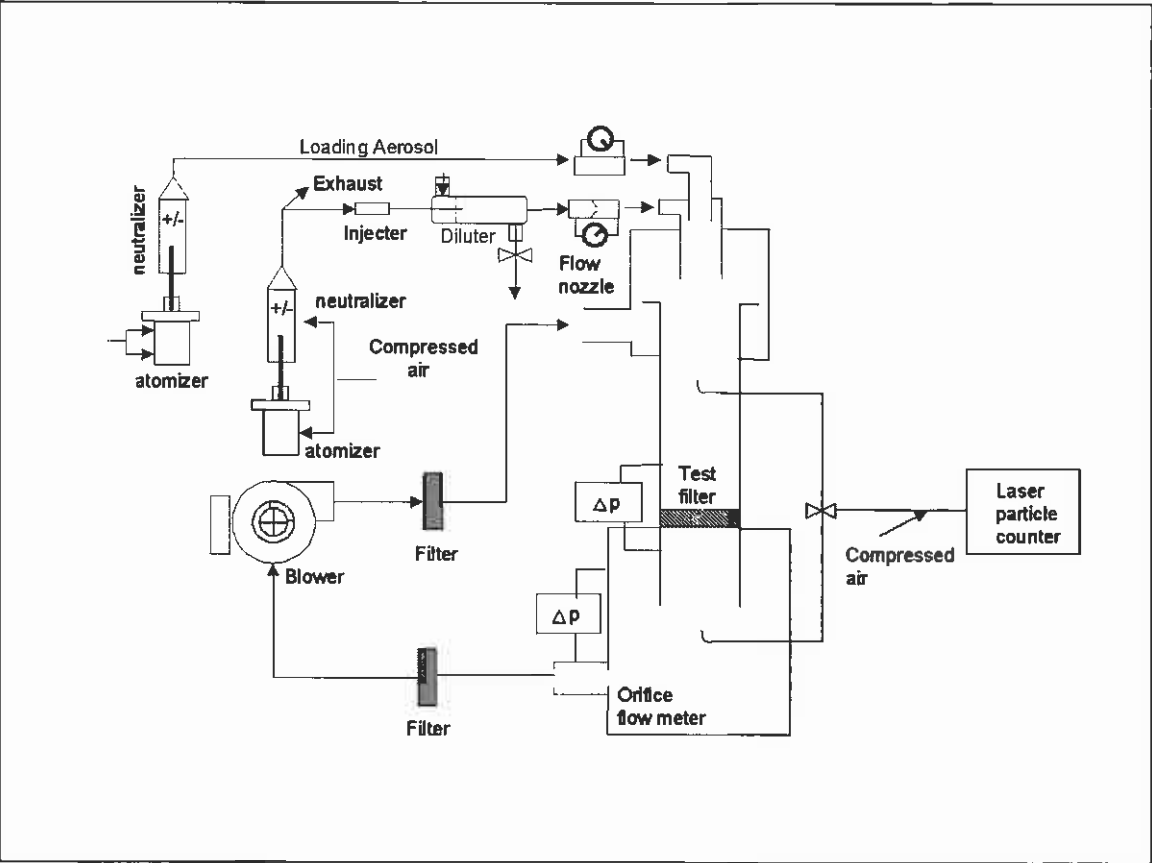
Figure 12. Liquid-Solid Contact Angle.

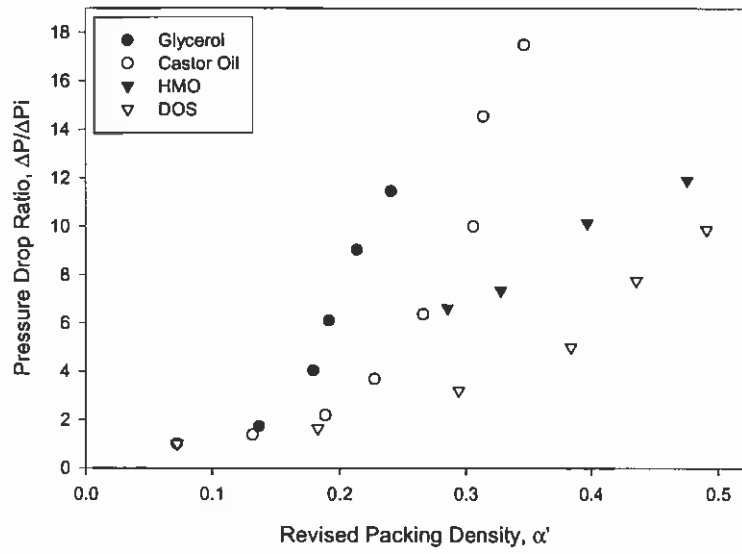
Figure 13. Three General Shapes Formed Between the Liquid and Fiber.

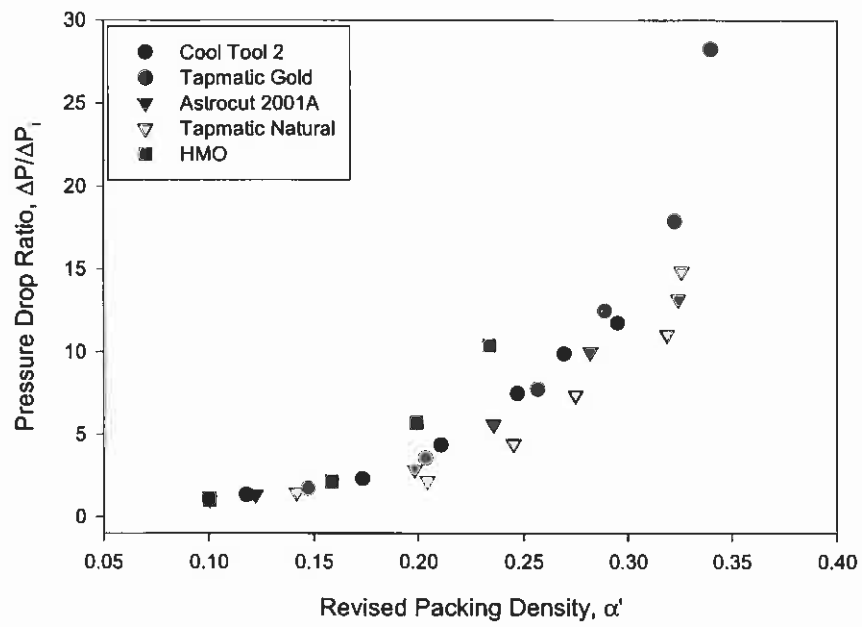
Figure 14. Summary of Liquid-Fiber Interactions.

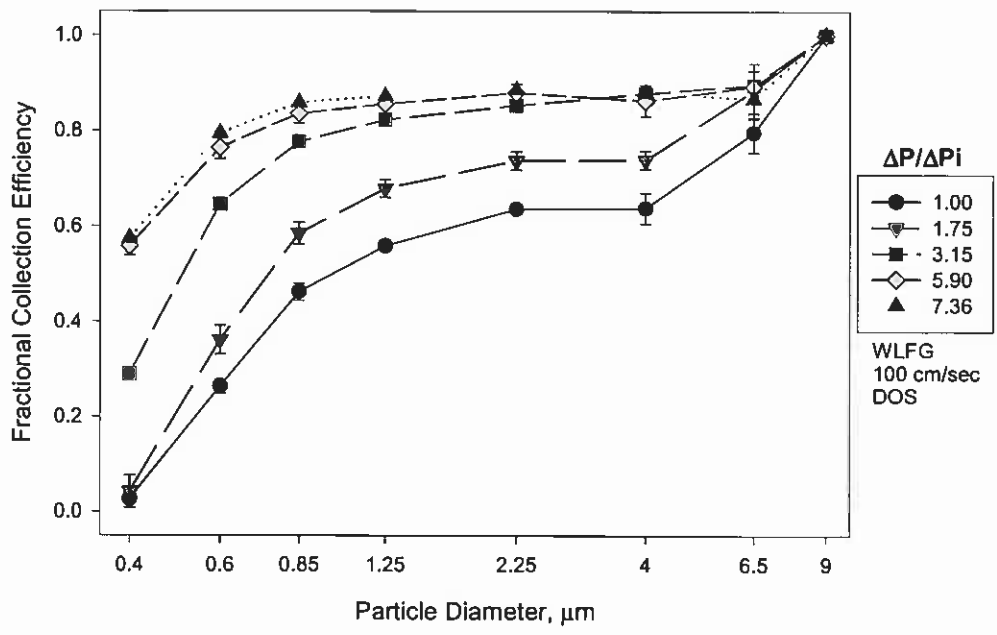
Figure 15. The Temporary Nature of the Drop in Collection Efficiency. (3 Filters loaded with DOS at 10 cm/sec).

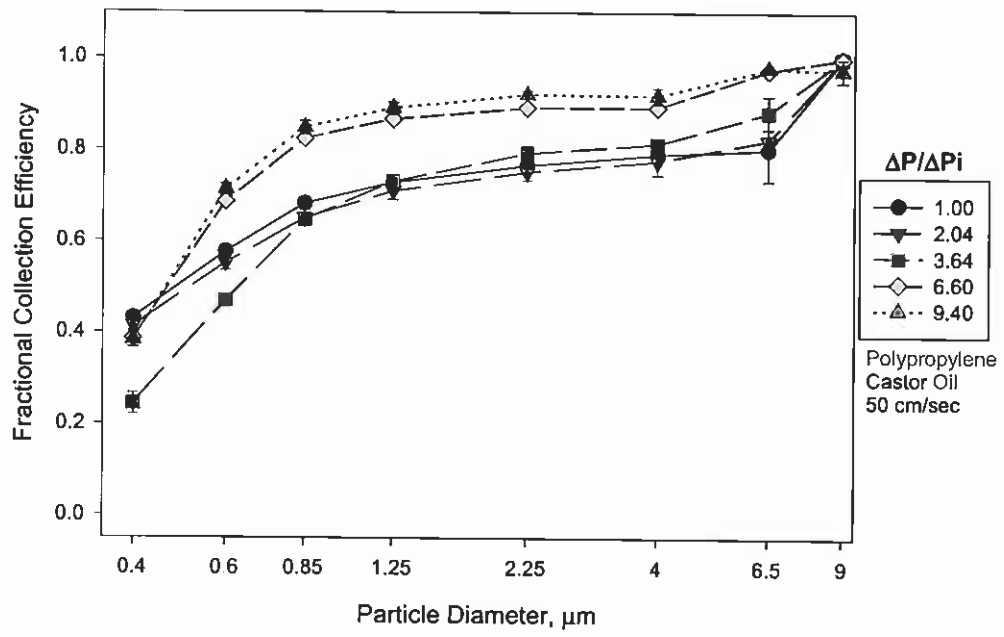
Figure 16. Three Different Polyester-Fiberglass Filters Loaded with DOS at 10 cm/sec. (Note that the Filter with the Lowest Packing Density has a Drop in Efficiency.)

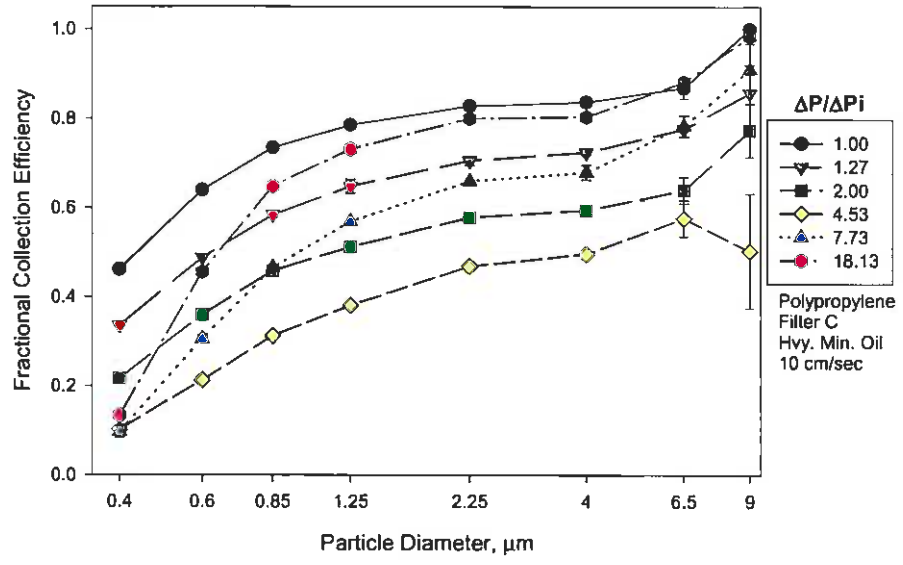


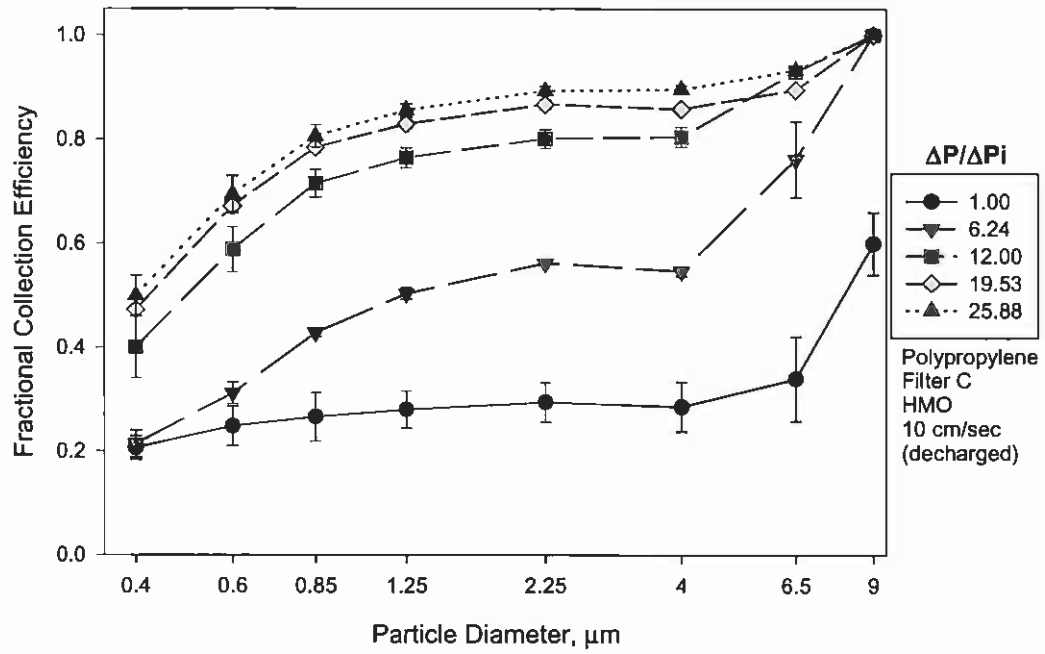


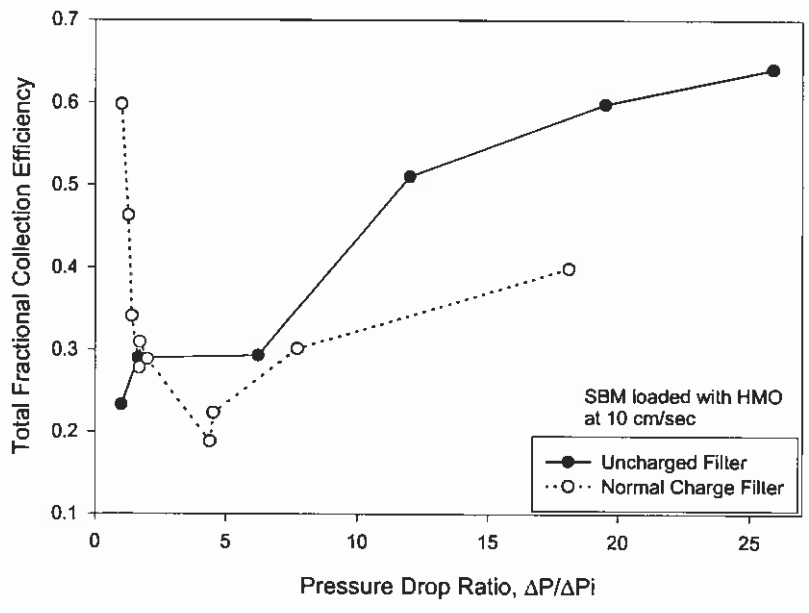


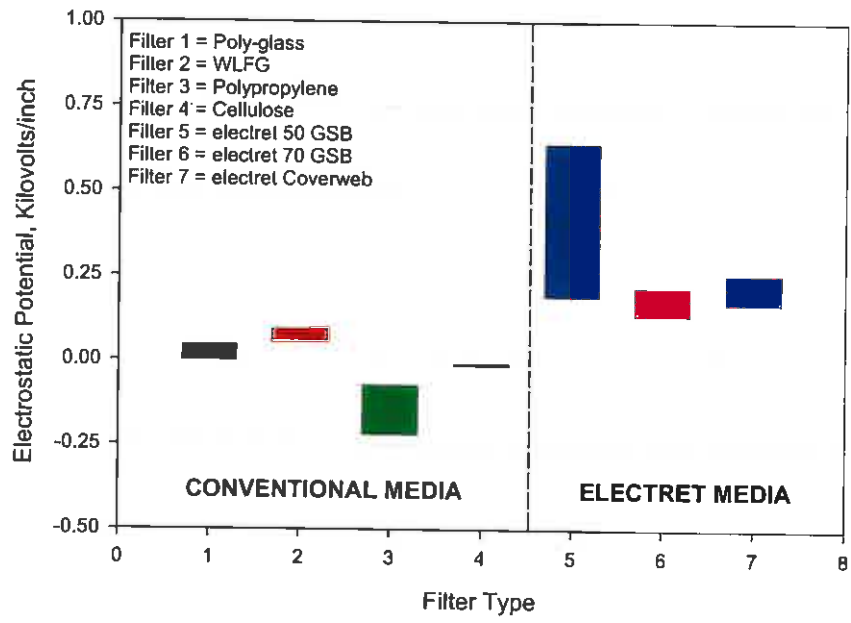


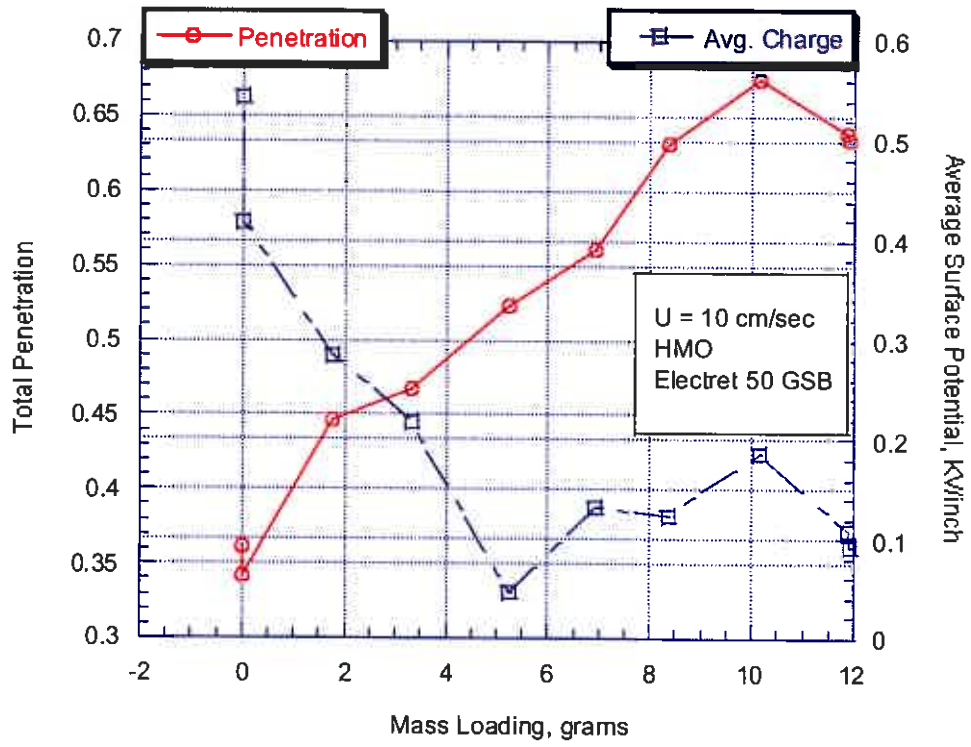


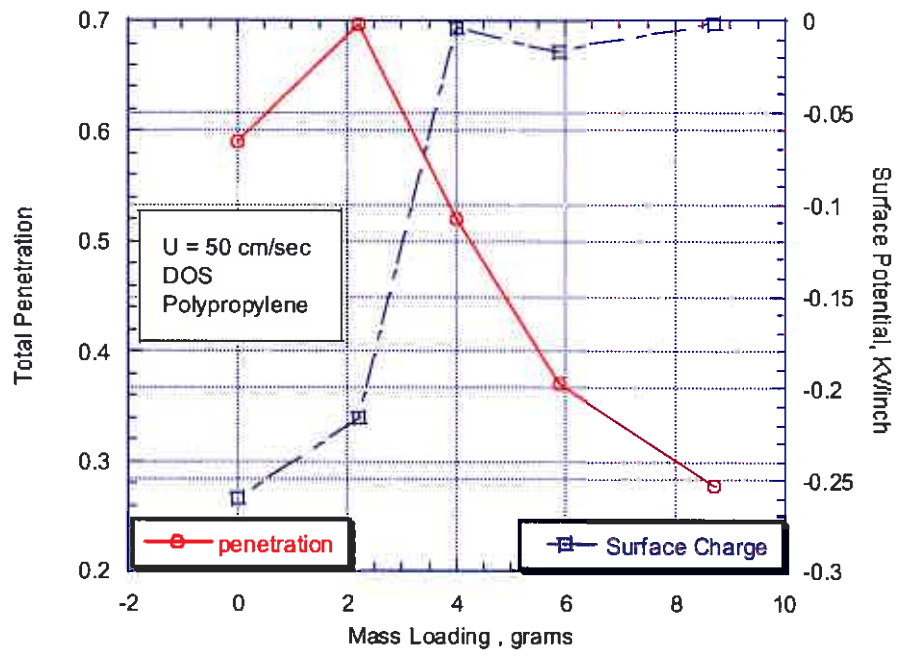




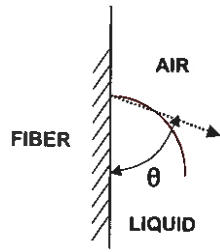




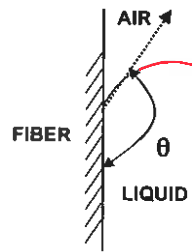




LIQUID-SOLID CONTACT ANGLE

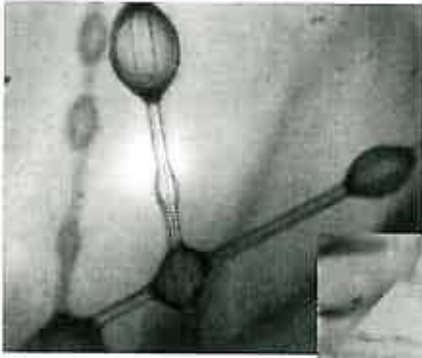


WETTING LIQUID



NONWETTING LIQUID

LIQUID FIBER INTERACTIONS (Three general shapes)



DOS ON FIBERGLASS
(UNDULOID)










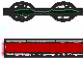



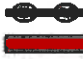




MWF ON FIBERGLASS
(COMPLETE COATING)




GLYCEROL ON POLYPROPYLENE
(CLAMSHELL)


LIQUID-FIBER INTERACTIONS

(Summary table)

	FIBERGLASS	POLY- PROPYLENE	POLYESTER/ GLASS	CELLULOSE
DOS				
HEAVY MINERAL OIL				
CASTOR OIL				
GLYCEROL				

 = COMPLETE WETTING

 = UNDULOID

 = CLAMSHELL

Temporary Nature of Drop in Collection Efficiency (3 Filters loaded with DOS at 10 cm/sec)

